Supporting Information

Recyclable switching between nonporous and porous phases of a square lattice (sql) topology coordination network

*Shi-Qiang Wang, Qing-Yuan Yang, Soumya Mukherjee, Daniel O'Nolan, Ewa Patyk-Kaźmierczak, Kai-Jie Chen, Mohana Shivanna, Claire Murray, Chiu C. Tang and Michael J. Zaworotko**

**E-mail:* Michael.Zaworotko@ul.ie

Table of Contents

Experimental Section

All materials were used as received from commercial sources.

Synthesis of square lattice (sql) coordination networks

$\{[Co(bipy)_2(NCS)_2]\cdot 2TFT\}_n$ (**sql-1-Co-NCS·2TFT**) was prepared by solvent diffusion method. In a typical procedure, a mixture of 2.5 mL ethanol and 2.5 mL *α*,*α*,*α*-trifluorotoluene (TFT) was slowly layered over 4,4′-bipyridine (0.3 mmol, 46.8 mg) dissolved in 5mL TFT. A solution of $Co(NCS)_2$ (0.15 mmol, 26.3 mg) in 5mL ethanol was filtered first and then carefully layered over the ethanol/TFT layer. The solution was left undisturbed for a few days to yield red prismatic crystals (79.6 mg, 68 %). The crystals were collected by filtration and washed with TFT three times. Crystals can retain single crystallinity over months when removed from mother liquor.

$[Co(bipy)_2(NCS)_2]_n$ (**sql-1-Co-NCS**) can be prepared by heating **sql-1-Co-NCS·2TFT** at 45 ºC overnight under vacuum. The prepared **sql-1-Co-NCS** still exhibits moderate single crystallinity that is enough for single crystal X-ray diffraction measurement.

$\{[Co(bipy)_2(NCS)_2]\cdot 3CO_2\}_n$ (**sql-1-Co-NCS·3CO_2**) can be formed within two hours by exposing **sql-1-Co-NCS** to CO_2 (195 K, 1 bar). **sql-1-Co-NCS·3CO_2** can transform to **sql-1-Co-NCS** when kept under ambient conditions.

Structural Studies of square lattice (sql) coordination networks

Single Crystal X-ray Diffraction

Suitable single crystals of all compounds were chosen for single crystal X-ray diffraction measurements. The data was collected on a Bruker D8 Quest diffractometer equipped with a IμS micro-focus Cu anode (λ = 1.54178 Å) and Photon II detector, or MoK_α source (λ = 0.71073 Å) and Photon 100 detector. For low temperature measurements, open-flow nitrogen attachment from Oxford Cryosystem was used. In all cases, data was indexed, integrated and scaled in APEX3.[1] Absorption correction was performed by multi-scan method using SADABS.[2] Space groups were determined using XPREP[3] implemented in APEX3. Structures were solved using intrinsic phasing method (SHELXT)[4] and refined on F^2 using nonlinear least-squares techniques with SHELXL[5] contained in OLEX2 v1.2.8 programs packages[6]. All non-hydrogen atoms were refined anisotropically. Hydrogen atoms were located from the molecular geometry at idealized positions and assigned isotropic thermal parameters depending on the equivalent displacement parameters of their carriers. Crystallographic data for the **sql** coordination networks are summarized in Table S1. All crystal structures have been deposited with the Cambridge Crystallographic Data Centre (CCDC 1818652-1818654).

Synchrotron Powder X-ray Diffraction

Synchrotron powder X-ray diffraction data was obtained from beamline I11 at the Diamond Light Source (λ = 0.82525(10) Å and zero point = 0.001050(3)°). Powder sample sealed in a Φ=0.5 mm capillary tube was measured at 195K under vacuum using five seconds scan and positional scanning detector (PSD) as well as 120 seconds scan and multi-analysing crystal-detectors (MACs). After that, CO_2 (195K, 1 bar) was filled in the capillary tube and powder X-ray data (PXRD) was collected again, after sample stabilised, by using multi-analysing crystal-detectors (MACs) and 1800 seconds exposure. The latter data set was used for structure

solution and refinement of **sql-1-Co-NCS·3CO$_2$**. Analysis of the powder data was carried out in GSAS-II;[7] the crystal structure of **sql-1-Co-NCS** was used as an original template. Lattice parameters were determined and structure factors obtained using the Pawley method. Atomic positions were found by the charge flipping method. The position for CO_2 guests could not be directly found and the number of guest molecules per unit could be determined by CO_2 sorption data. Crystallographic data is summarized in Table S2 and comparative patterns for the observed and calculated intensities including their differences are presented in Figure S1.

Characterization and Property Studies of square lattice (sql) coordination networks

Powder X-ray Diffraction

Powder X-ray diffraction experiments were conducted using microcrystalline samples on a Panalytical Empyrean diffractometer (40 kV, 40 mA, Cu K$\alpha_{1,2}$, λ = 1.5418 Å) in Bragg-Brentano geometry. A scan speed of 0.111747˚/s (6.7˚/min), with a step size of 0.026˚ in 2θ was used at room temperature with a range of 5˚< 2θ < 40˚.

Variable temperature Powder X-ray Diffraction (VT-PXRD)

For VT-PXRD experiments, reflections were collected on Panalytical X'Pert diffractometer (40 kV, 40 mA, Cu K$\alpha_{1,2}$, λ = 1.5418 Å) at 10 ºC intervals from 30 to 210 ºC by heating at 1 ºC/min under N_2 atmosphere. Water cooling system was adopted to control the temperature. Diffraction patterns were collected in the 2θ range of 5-40º.

Thermogravimetric Analysis (TGA)

TGA for all the compounds were carried out under N_2 atmosphere in a TA instruments Q50 thermal analyzer between room temperature and 550 ˚C with a constant heating rate of 10 ºC/min.

Low Pressure Gas Adsorption Studies

Low pressure gas adsorption experiments (up to 1 bar) of **sql-1-Co-NCS** were conducted on a Micromeritics TriStar II PLUS 3030 instrument (77 K N_2 and 195 K CO_2). Samples of **sql-1-Co-NCS·2TFT** were degassed under vacuum at 45 ˚C overnight to transform to **sql-1-Co-NCS** by using a Smart VacPrep instrument prior to the analysis. 77 K for the N_2 sorption experiments were maintained with a 4 L Dewar flask filled with liquid N_2, whereas 195K CO_2 experiments were maintained with a 4 L Dewar flask filled with the mixture of acetone and dry ice.

High Pressure Gas Adsorption Studies

High pressure CO_2 isotherms of **sql-1-Co-NCS** were collected on a Micromeritics HPVA II-100 instrument at different temperatures (in the range 253K-298 K). Samples of **sql-1-Co-NCS·2TFT** were loaded into a tared stainless steel sample holder and degassed on Micromeritics Smart VacPrep instrument until the outgas rate was less than 0.003 mbar/min. The sample holder with degassed sample (*ca.* 300mg) was then transferred to the HPVA II-100, connected to the instrument's analysis port via an OCR fitting, and evacuated at room temperature for 1 hour before the measurements. Free spaces were determined at 0.7 bar Helium (He) and 25 ˚C. A background correction was performed by subtracting the adsorption of the empty cell from the obtained

isotherms. Notably, the average CO_2 uptakes (127 cm^3/g) are slightly lower than those collected at 195 K and 1 bar (136 cm^3/g), may due to the relatively low precision of the HPVA equipment.

Recyclability Studies

The recyclability tests for **sql-1-Co-NCS** were also recorded using the Micromeritics HPVA II-100 instrument at 273 K. To optimize the time efficiency, 10 data points were set for each cycle that needs *ca.* 50 mins. Due to the limitation of the equipment, 100 cycles of CO_2 sorption isotherms were collected over 10 runs (10 cycles per run). Because every 10 cycles were collected continuously, i.e. the last data point of previous cycle is the starting data point of next cycle, the background undergoes a gradual increment which was subtracted for each cycle.

Vacuum Dynamic Vapor Sorption

Dynamic water vapor sorption measurements were conducted using a Surface Measurement Systems DVS Vacuum at 303 K. Samples of **sql-1-Co-NCS** were further degassed under high vacuum ($2x10^{-6}$ Torr) *in-situ* and stepwise increase in relative pressure were controlled by equilibrated weight changes of the sample (dM/dT = 0.006 %/min) from 0 to 90%. Vacuum pressure transducers were used with ability to measure from $1x10^{-6}$ to 760 Torr with a resolution of 0.01%. Approximately 15 mg of sample was used for the experiment. The mass of the sample was determined by comparison to an empty reference pan and recorded by a high resolution microbalance with a precision of 0.1 μg.

Table S1. Crystallographic data of square lattice (**sql**) coordination networks.

	sql-1-Co-NCS·2TFT	**sql-1-Co-NCS**
Formula	$C_{36}H_{26}CoF_6N_6S_2$	$C_{22}H_{16}CoN_6S_2$
Formula weight	779.68	487.46
Temperature/K	273	100
Crystal system	Monoclinic	Monoclinic
Space group	*C*2/*c*	*C*2/*c*
a/Å	23.3527(13)	12.099(4)
b/Å	11.5209(7)	11.399(3)
c/Å	13.7802(9)	16.538(5)
β/°	108.764(2)	99.939(13)
Volume/Å^3	3510.4(4)	2246.6(11)
Z	4	4
ρ_{calc} g/cm^3	1.475	1.441
μ/mm^{-1}	0.676	7.899
F(000)	1588.0	996.0
Radiation	MoKα	CuKα
Reflections collected	33663	2382
Independent reflections	3725 [R_{int} = 0.0532, R_{sigma} = 0.0373]	818 [R_{int} = 0.0804, R_{sigma} = 0.0910]
Data/restraints/parameters	3725/52/253	818/110/143
Goodness-of-fit on F^2	1.053	1.158
Final R indexes	R_1 = 0.0594,	R_1 = 0.1345,
[I>=2σ (I)]	wR_2 = 0.1408	wR_2 = 0.3363
Final R indexes	R_1 = 0.0920,	R_1 = 0.1586,
[all data]	wR_2 = 0.1599	wR_2 = 0.3577

Table S2. Crystallographic data of **sql-1-Co-NCS·3CO$_2$** refined from synchrotron powder X-ray diffraction.

	sql-1-Co-NCS·3CO$_2$
Formula	$C_{25}H_{16}O_6CoN_6S_2$
Formula weight	619
Crystal system	monoclinic
Space group	*C2/c*
a/Å	12.605016
b/Å	11.467969
c/Å	19.683948
β/°	92.9158
Volume/Å^3	2841.71
R/%	3.03
Rexp/%	0.67
RF/%	1.71
RF^2/%	8.05
wRp/%	5.96
Goodness-of-fit	8.91

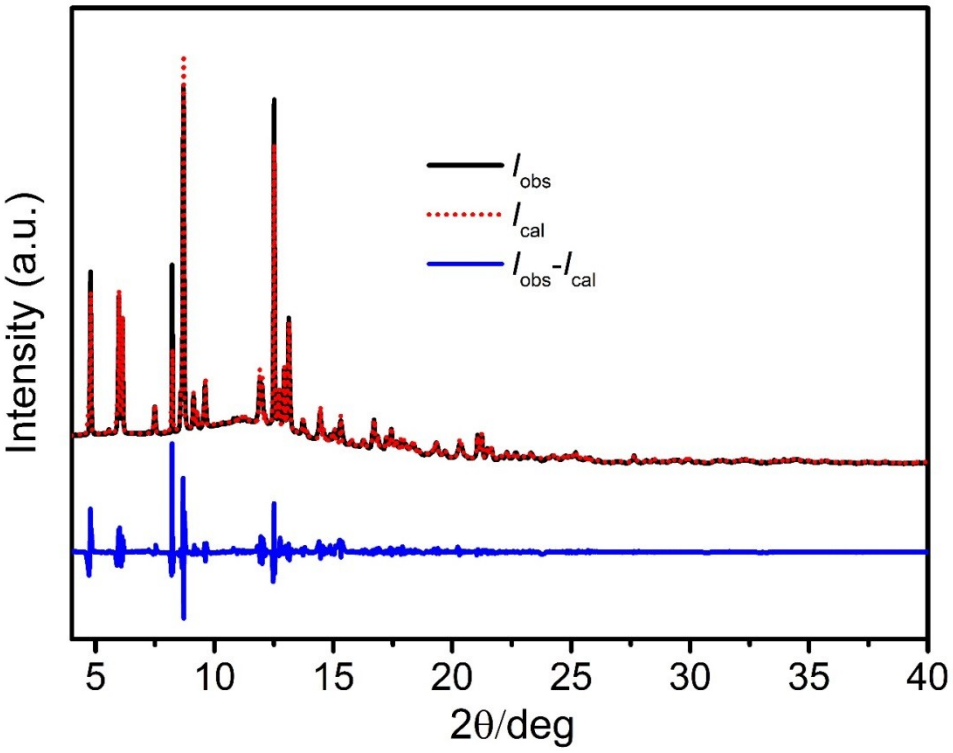

Figure S1. Synchrotron powder X-ray patterns for **sql-1-Co-NCS·3CO$_2$** (black), the calculated pattern for the resolved structure (red), and a difference plot of the observed and calculated intensities (blue).

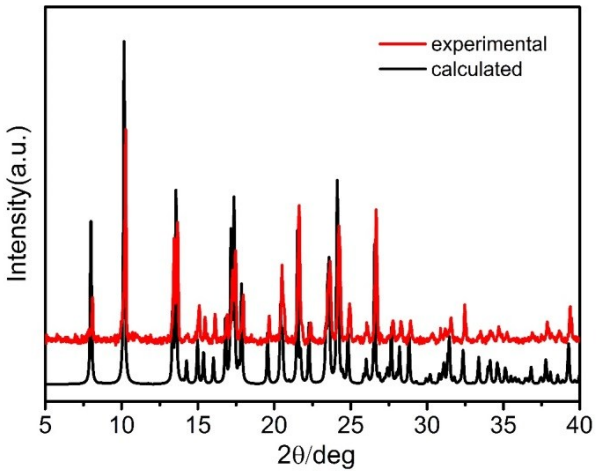

Figure S2. The PXRD patterns of **sql-1-Co-NCS·2TFT**.

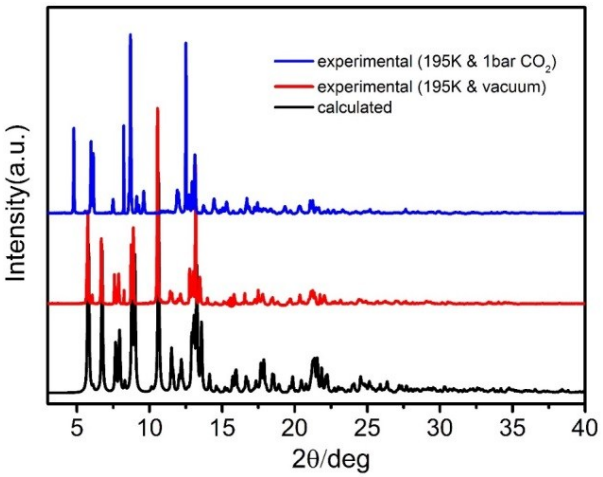

Figure S3. The synchrotron PXRD patterns of **sql-1-Co-NCS**.

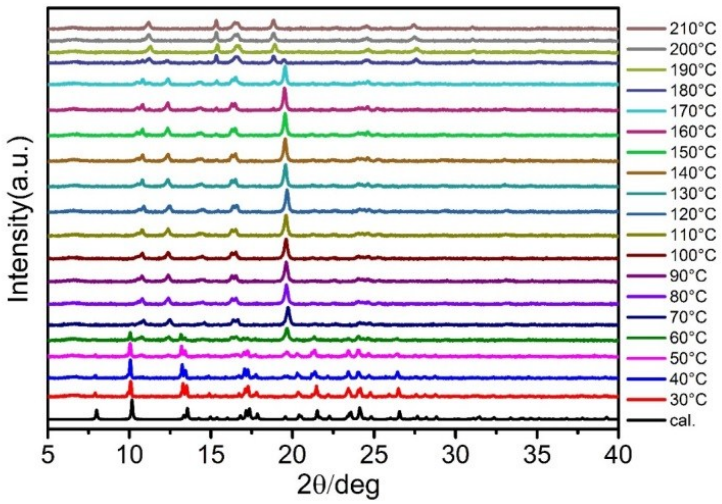

Figure S4. The VT-PXRD patterns of **sql-1-Co-NCS·2TFT**.

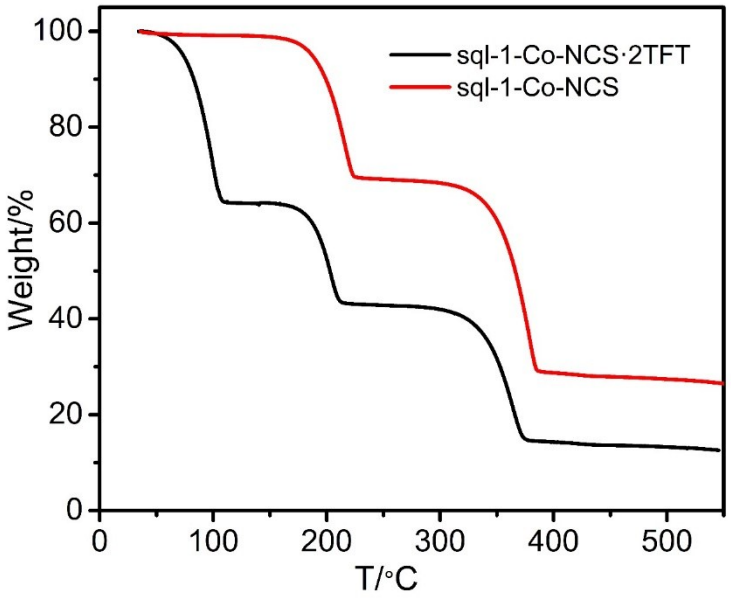

Figure S5. TGA profiles for **sql-1-Co-NCS·2TFT** and **sql-1-Co-NCS**.

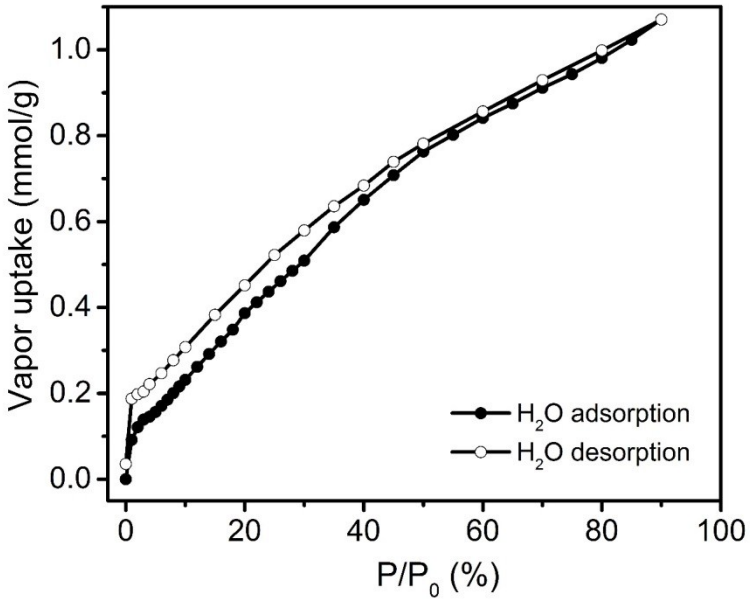

Figure S6. Dynamic water vapour sorption for **sql-1-Co-NCS** at 303 K.

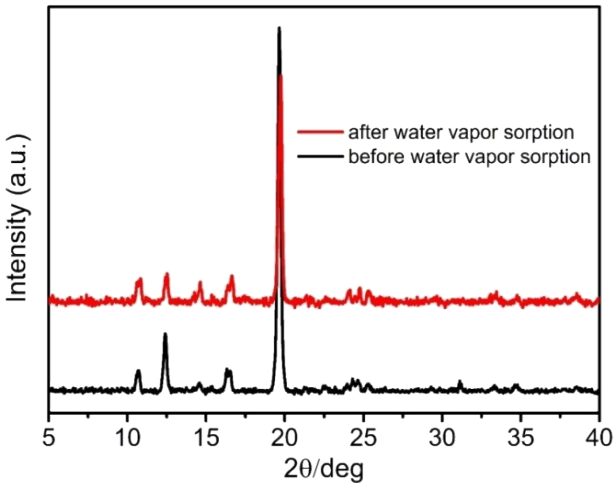

Figure S7. Comparison of PXRD patterns of **sql-1-Co-NCS** before (black) and after (red) water vapour sorption.

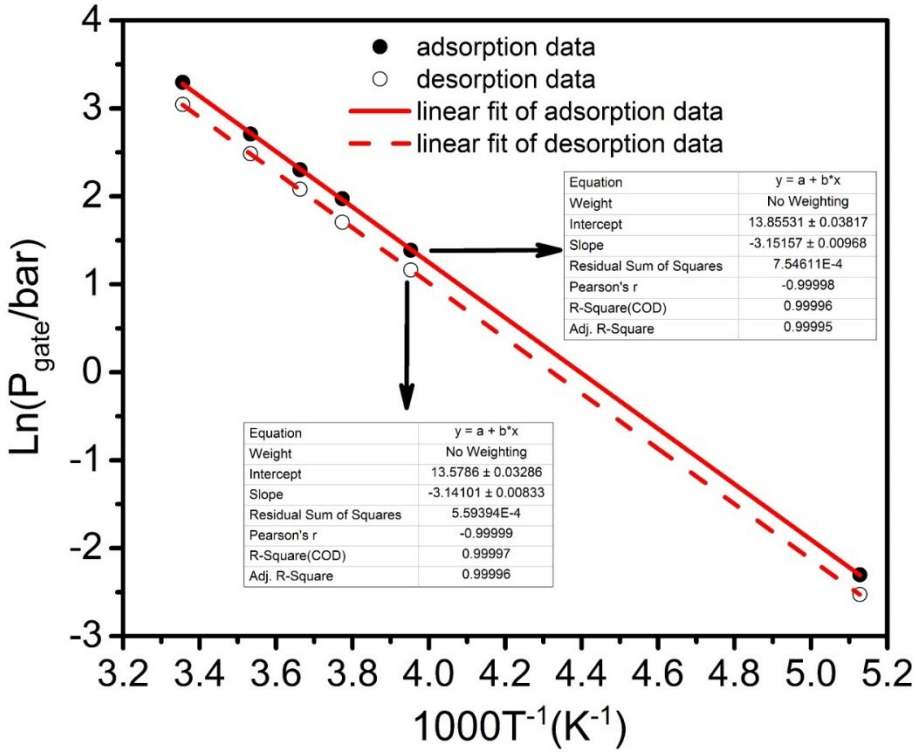

Figure S8. The temperature dependence of switching pressure based on CO_2 sorption data of **sql-1-Co-NCS**.

Depending on Clausius-Clapeyron equation: $d\ln P/(d(1/T)) = \Delta H/R$, where P is switching pressure, T is measurement temperature, R is gas constant, the linear fits for both branches of the sorption data are in excellent accord to lead us to their correlation equations: $\ln(P_{ga}/\text{bar}) = -3152/T + 13.86$; $\ln(P_{gd}/\text{bar}) = -3141/T + 13.58$. Thus the formation enthalpy of the clathrate $\Delta_f H$ is *ca.* 26.2 kJ/mol and the corresponding dissociation enthalpy of the clathrate $\Delta_d H$ is *ca.* 26.1 kJ/mol.

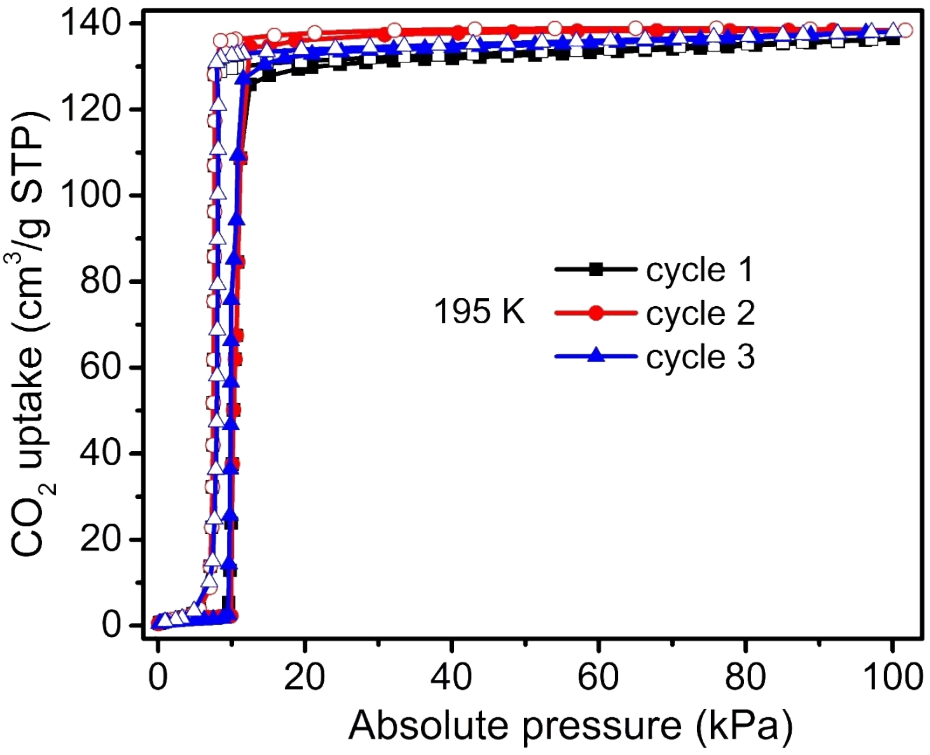

Figure S9. Recyclability test of low-pressure CO_2 sorption for **sql-1-Co-NCS** at 195 K.

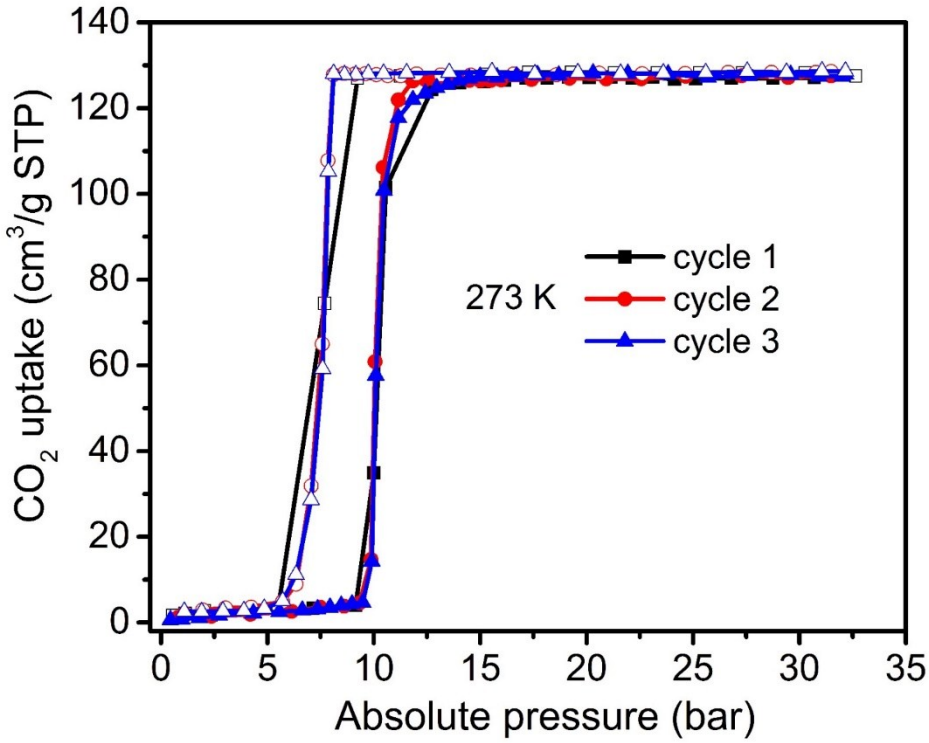

Figure S10. Recyclability test of high-pressure CO_2 sorption for **sql-1-Co-NCS** at 273 K.

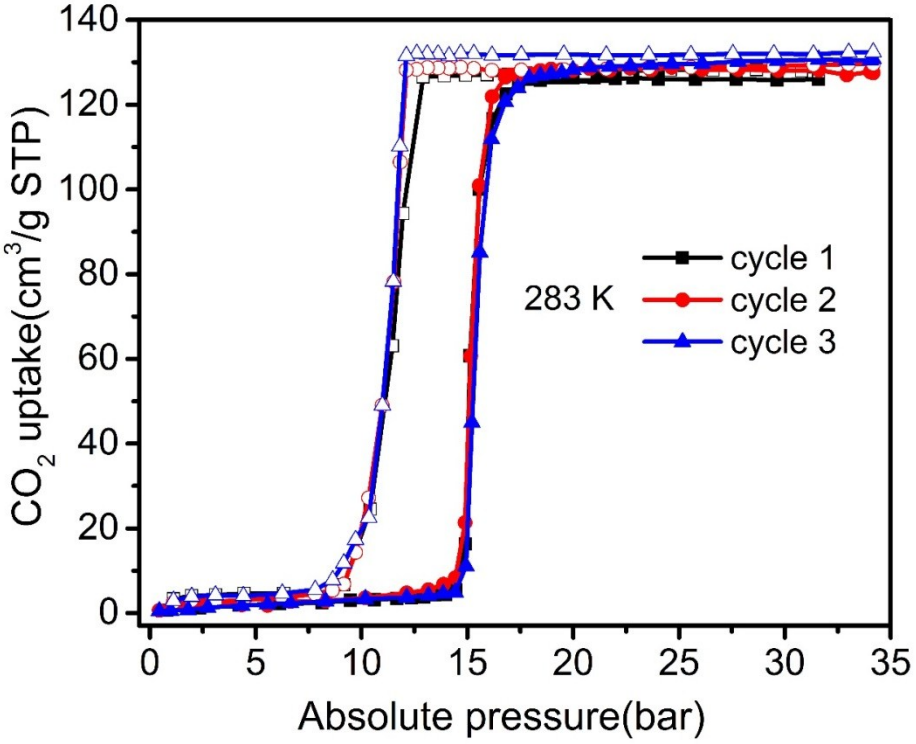

Figure S11. Recyclability test of high-pressure CO_2 sorption for **sql-1-Co-NCS** at 283 K.

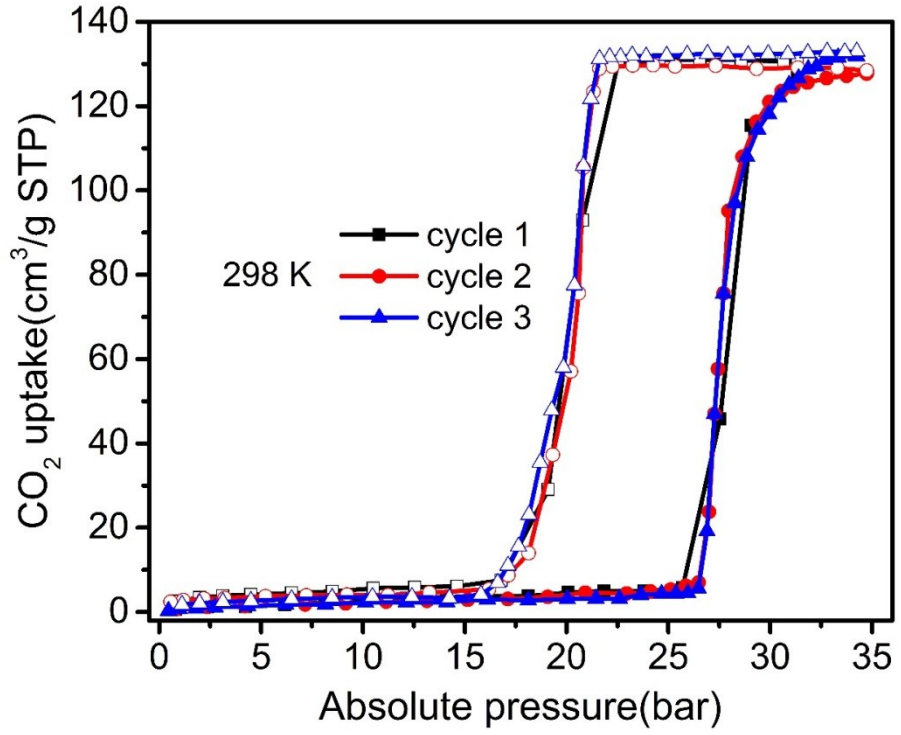

Figure S12. Recyclability test of high-pressure CO_2 sorption for **sql-1-Co-NCS** at 298 K.

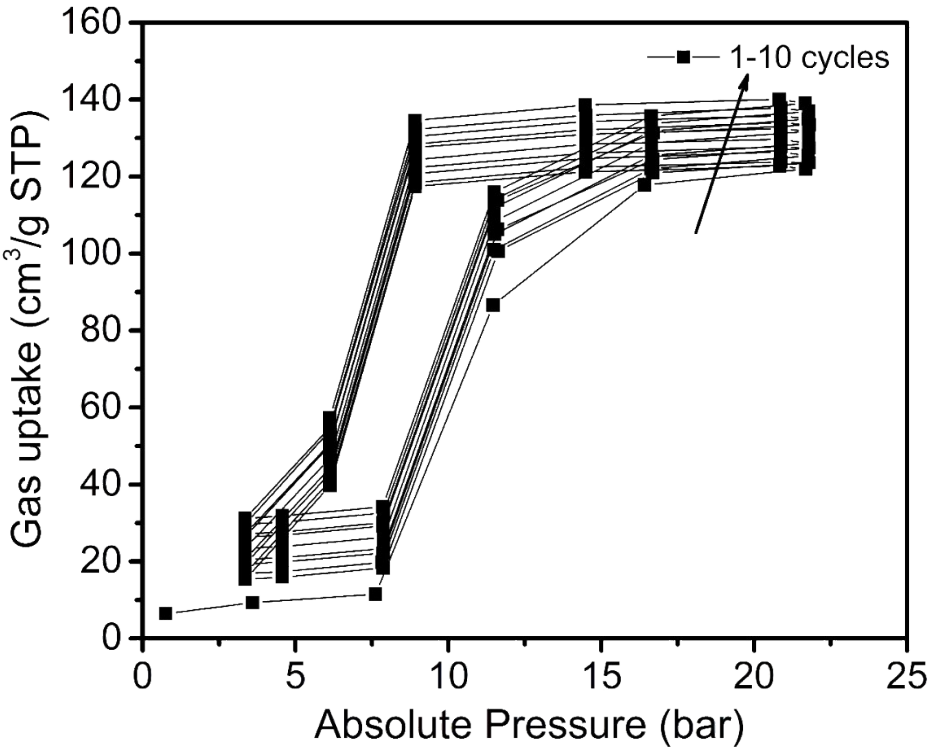

Figure S13. Recyclability test (1-10 cycles) of high-pressure CO_2 sorption for **sql-1-Co-NCS** at 273 K.

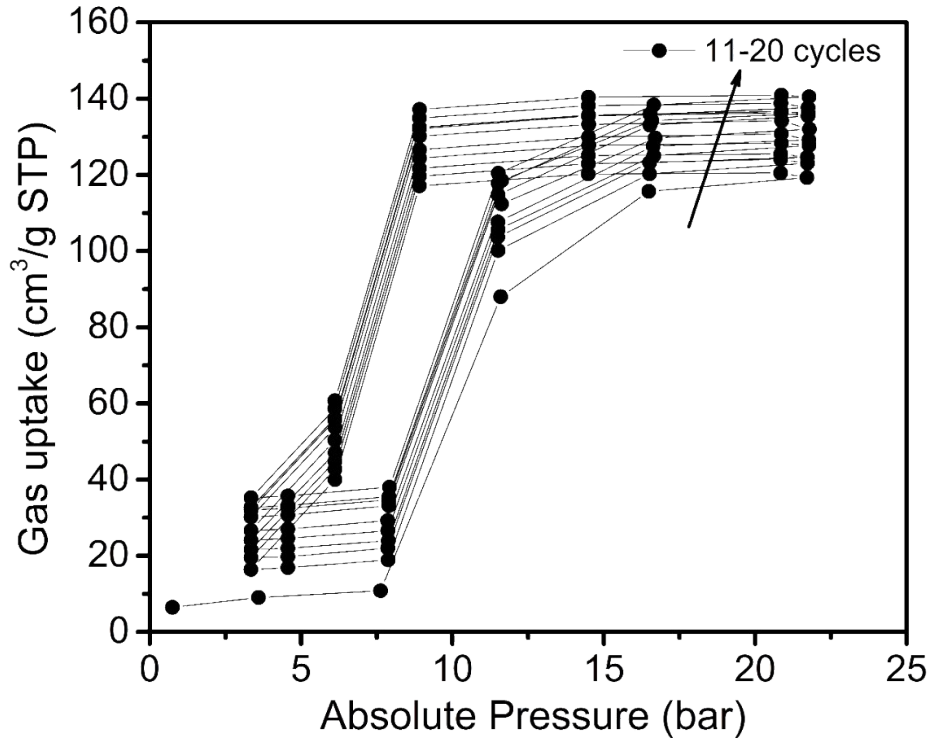

Figure S14. Recyclability test (11-20 cycles) of high-pressure CO_2 sorption for **sql-1-Co-NCS** at 273 K.

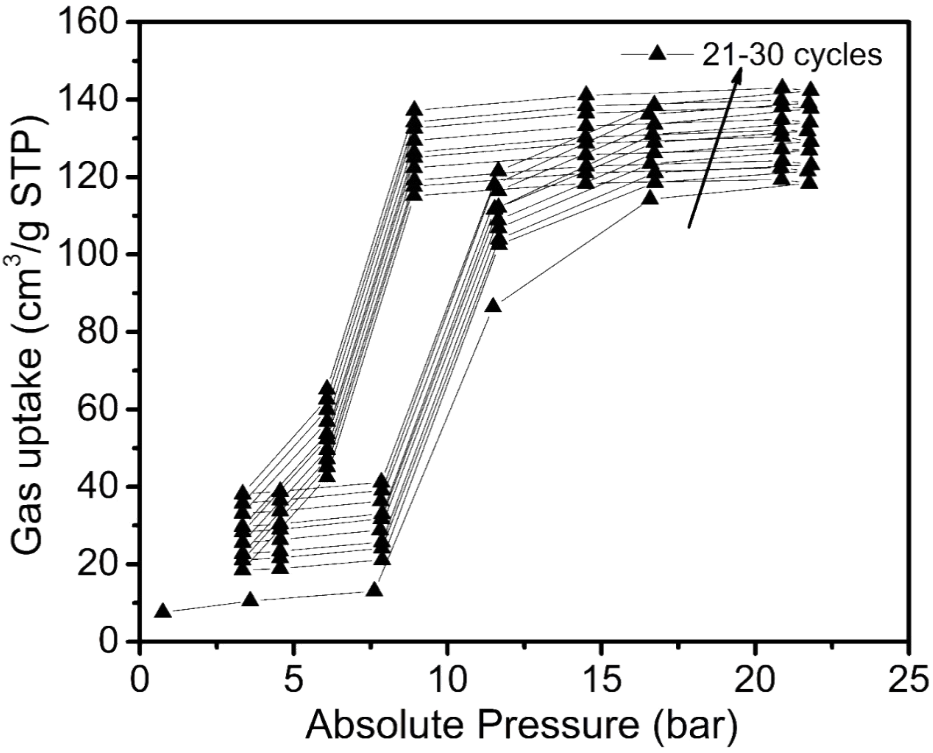

Figure S15. Recyclability test (21-30 cycles) of high-pressure CO_2 sorption for **sql-1-Co-NCS** at 273 K.

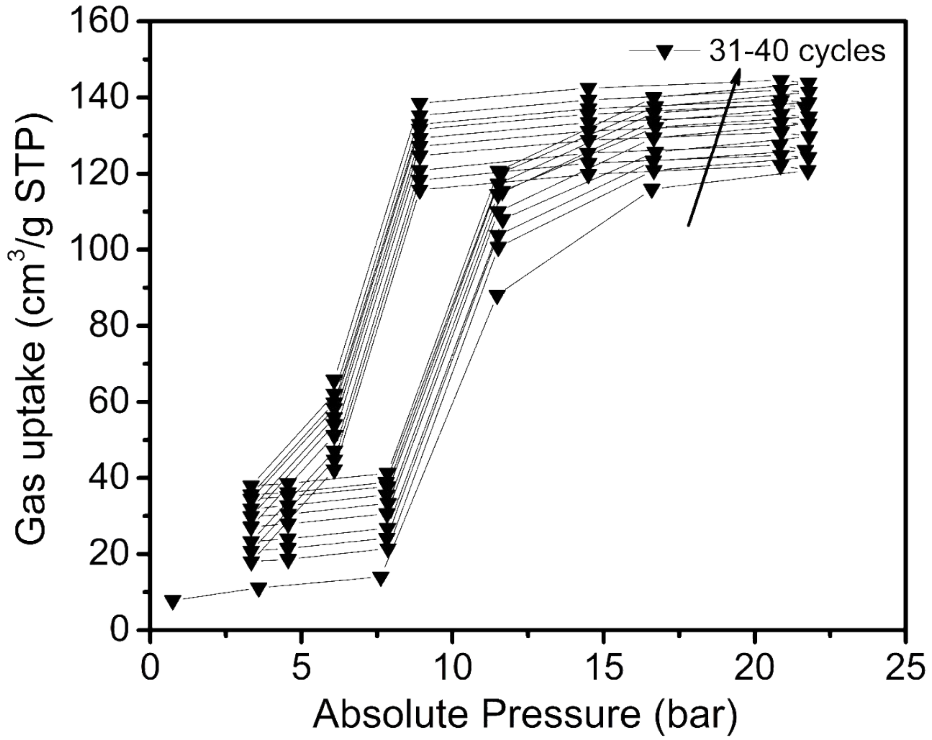

Figure S16. Recyclability test (31-40 cycles) of high-pressure CO_2 sorption for **sql-1-Co-NCS** at 273 K.

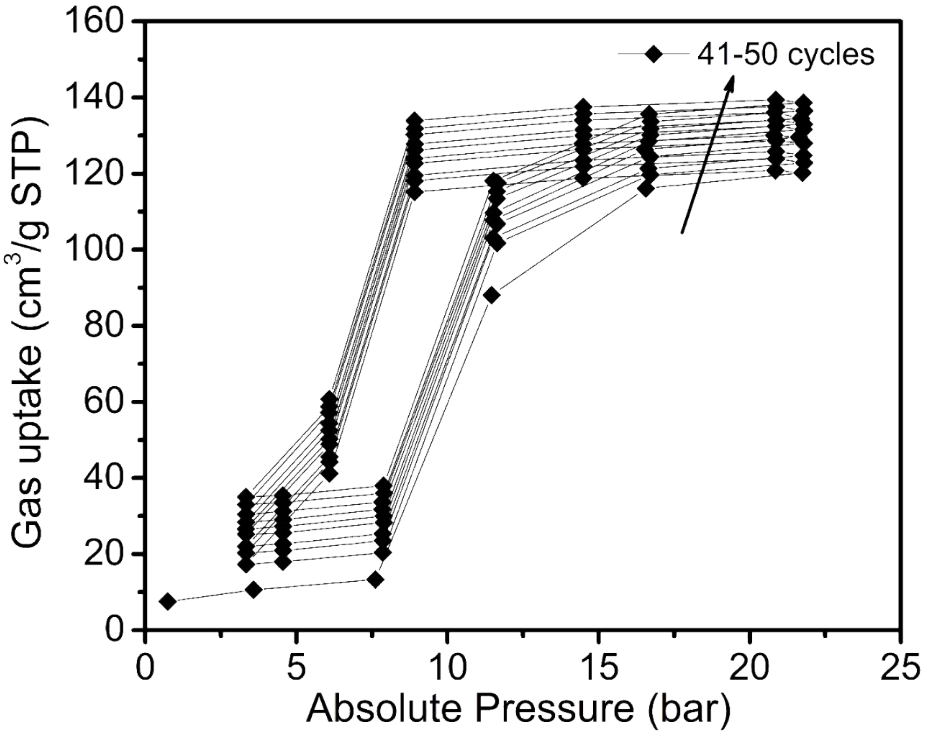

Figure S17. Recyclability test (41-50 cycles) of high-pressure CO_2 sorption for **sql-1-Co-NCS** at 273 K.

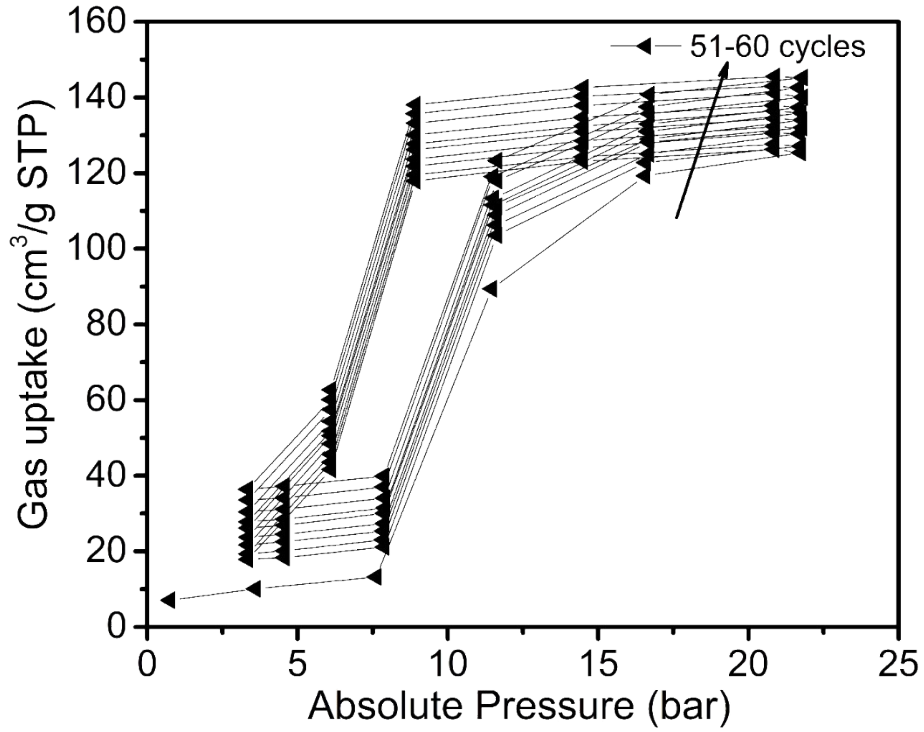

Figure S18. Recyclability test (51-60 cycles) of high-pressure CO_2 sorption for **sql-1-Co-NCS** at 273 K.

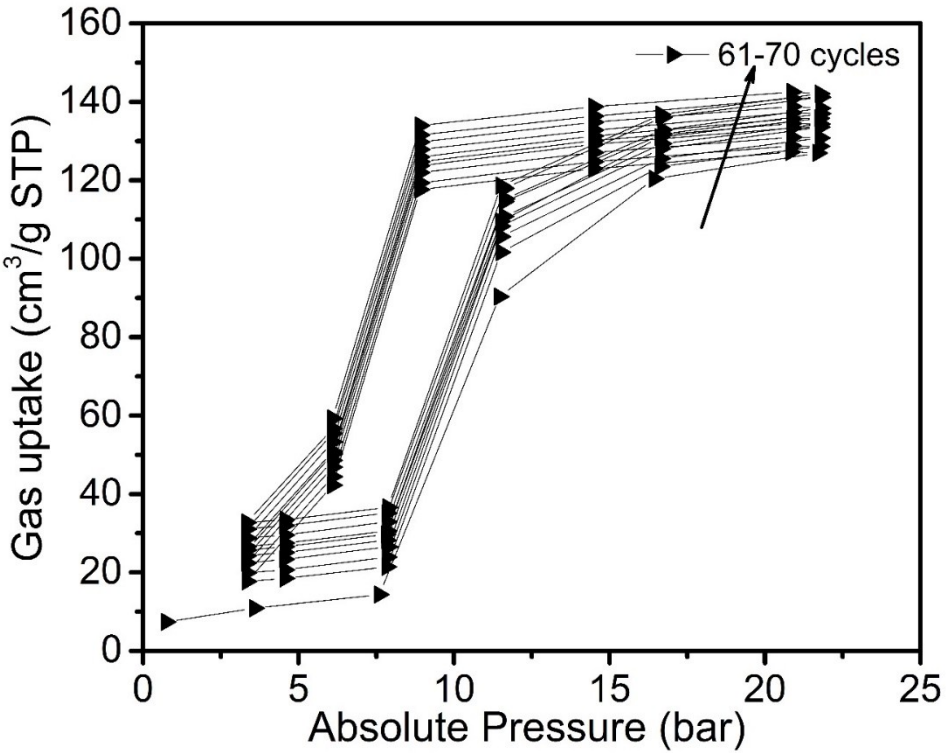

Figure S19. Recyclability test (61-70 cycles) of high-pressure CO_2 sorption for **sql-1-Co-NCS** at 273 K.

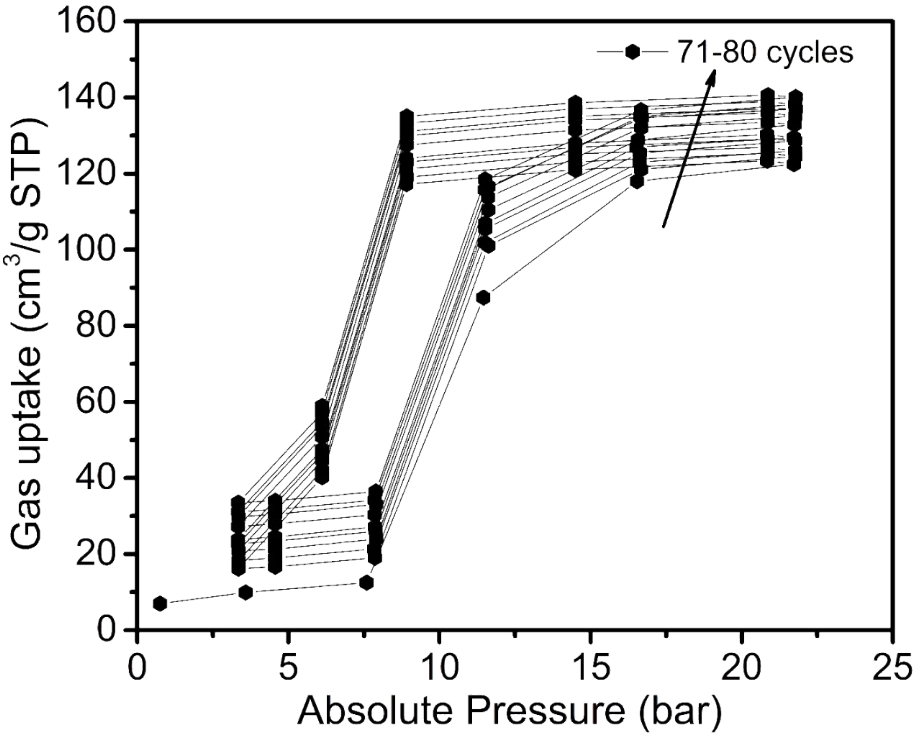

Figure S20. Recyclability test (71-80 cycles) of high-pressure CO_2 sorption for **sql-1-Co-NCS** at 273 K.

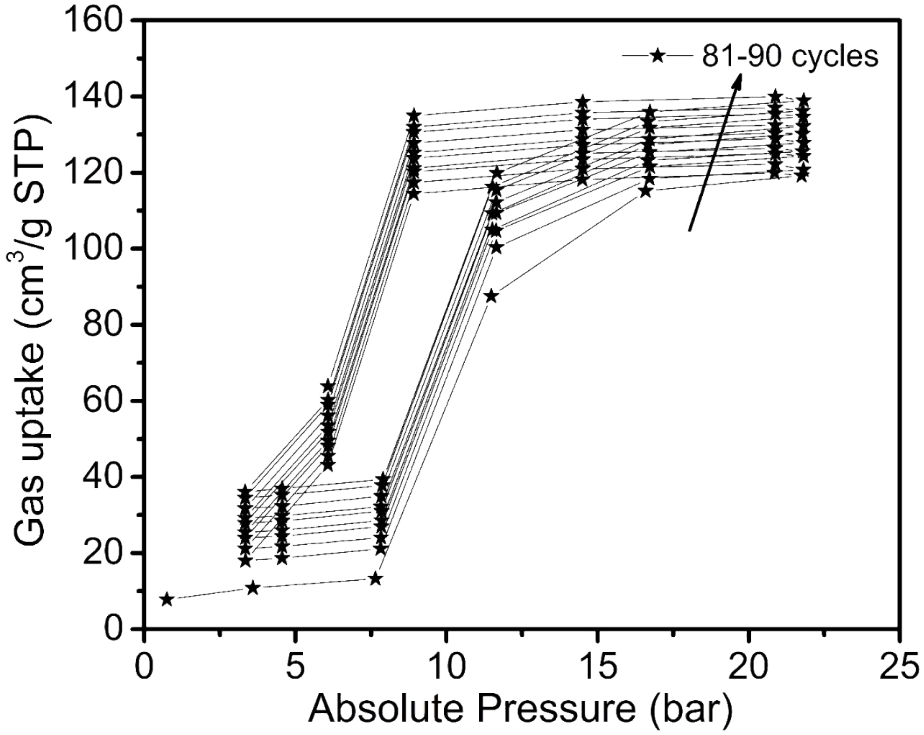

Figure S21. Recyclability test (81-90 cycles) of high-pressure CO_2 sorption for **sql-1-Co-NCS** at 273 K.

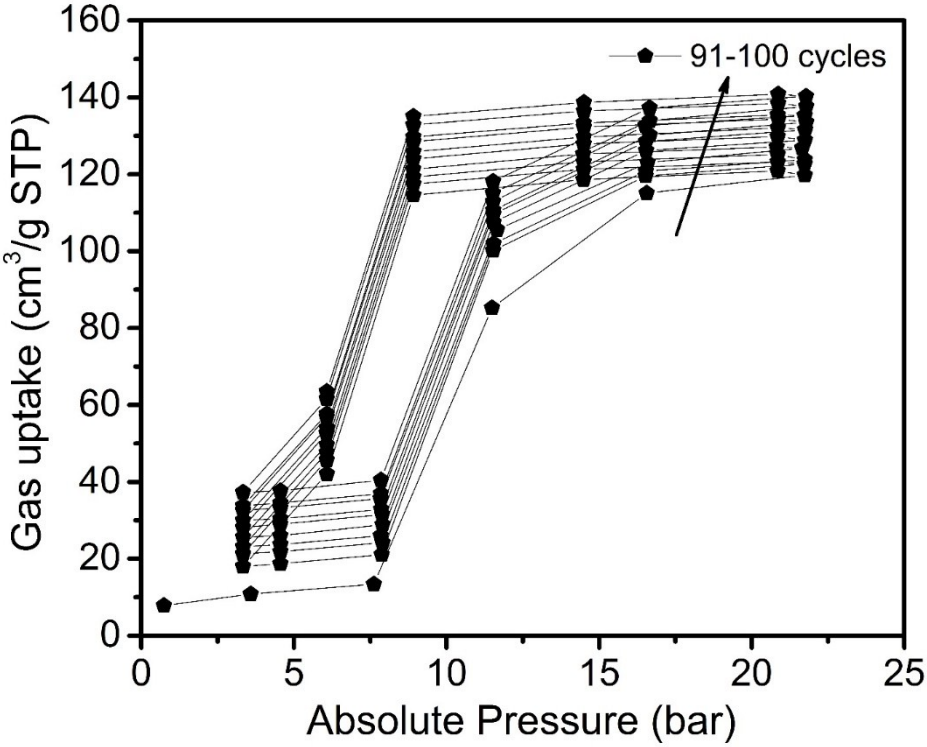

Figure S22. Recyclability test (91-100 cycles) of high-pressure CO_2 sorption for **sql-1-Co-NCS** at 273 K.

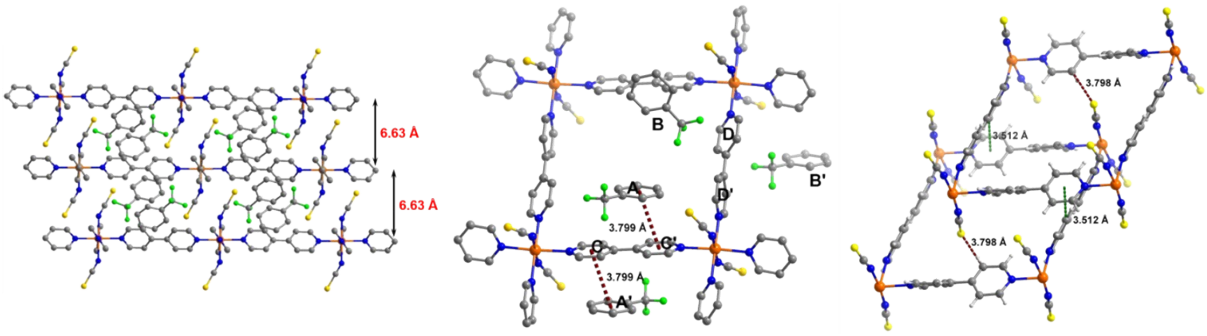

Figure S23. Left: Layer packing arrangement of **sql-1-Co-NCS·2TFT**; middle: The host-guest interactions in **sql-1-Co-NCS·2TFT**. B/B′ and A/A′ exhibit π···π interactions with the adjacent layers; right: Host-host interactions in **sql-1-Co-NCS** include C-H···S hydrogen bonds and C-H···π interactions.

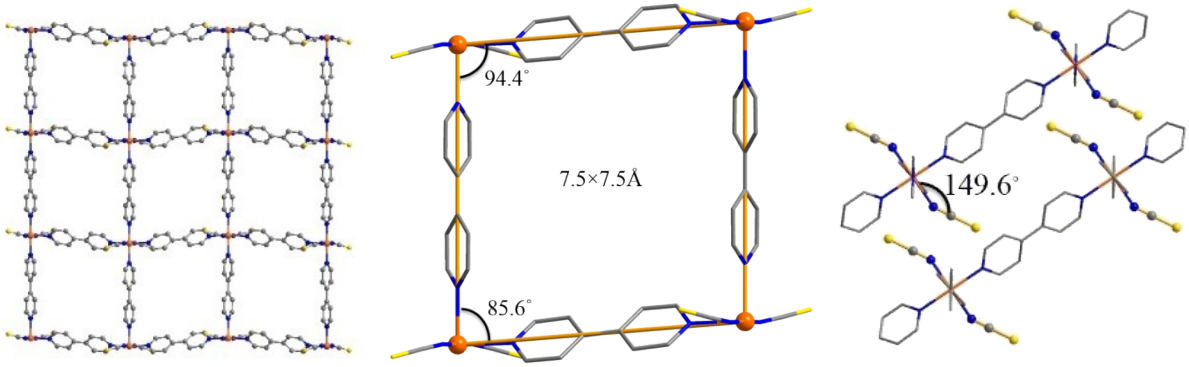

Figure S24. Crystal structure of **sql-1-Co-NCS·2TFT** depicting the square grids and layer packing.

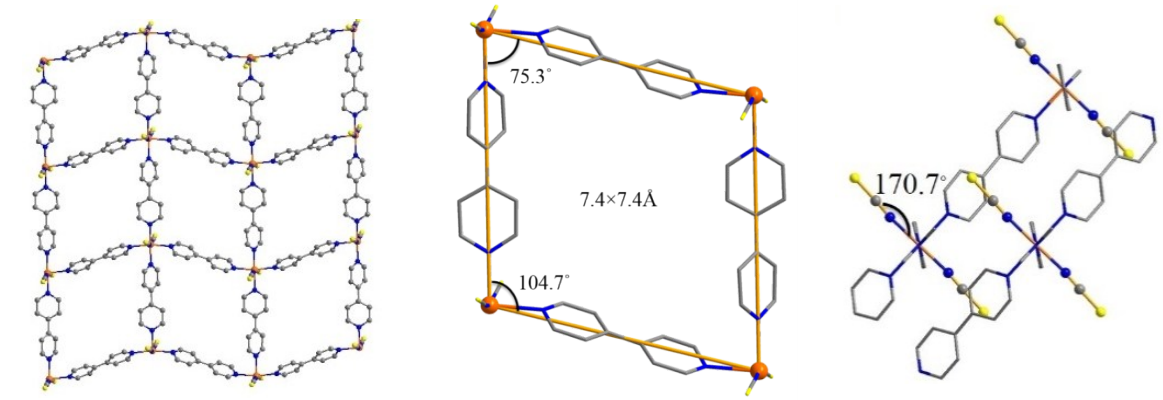

Figure S25. Crystal structure of **sql-1-Co-NCS** depicting the square grids and layer packing.

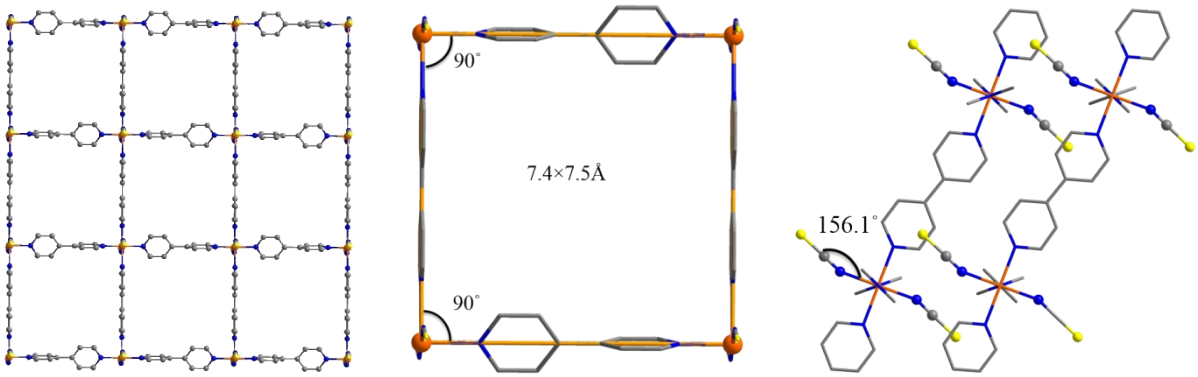

Figure S26. Crystal structure of **sql-1-Co-NCS·3CO$_2$** depicting the square grids and layer packing.

Table S3. Structural parameters of each **sql** network.

Compound	Square grid angles (°)[a]	∠Co-N-CS (°)	Torsion angle of bipy (°)	Interlayer separation (Å)
sql-1-Co-NCS (100 K)	75.3/104.7	170.9	50% (54.5); 50% coplanar	4.46
sql-1-Co-NCS·2TFT (273 K)	85.6/94.4	140.6	50% (43.6); 50% coplanar	6.63
sql-1-Co-NCS·3CO$_2$ (195 K)	90/90	156.1	50% (64.1); 50% coplanar	5.39

[a] The square grid angles refer to $\angle_{Co\text{-}Co\text{-}Co}$ angles

Table S4. Summary of switching materials from closed to open phases (single-step) with uptake > 100 cm^3/g.

Materials	Dimensional	Triggered gas	Uptake (cm^3/g)	Ref.
sql-1-Co-NCS	2D	CO_2	136 (195 K)	this work
DUT-8 (Ni)	3D	CO_2	590 (196 K)	8
[Zn(TCNQ–TCNQ)bpy]	3D	O_2, NO	268 (O_2, 77 K); 322 (NO, 121 K)	9
Fe(bdp)	3D	CH_4	295 (298 K)	10
Co(bdp)	3D	CH_4	246 (298 K)	
ELM-11	2D	N_2, CO_2,et al	260 (N_2, 77 K);76 (CO_2, 273 K)	11
MOF-508 analogue $[Zn(C_{20}H_{12}O_4)_2(C_{10}H_8N_2)]_n$	3D	CO_2	188 (298 K)	12
[Cd(bpndc)(bpy)]	2D	O_2, N_2, Ar	159 (O_2, 90 K);151 (N_2, 90 K);130 (Ar, 90 K)	13
$[Cu(CF_3SO_3)_2(bpp)_2]_n$	2D	CO_2	153 (195 K)	14
[Ni(bdc)(bphy)]·DMF·3.5H_2O	2D	CO_2	147 (298 K)	15
f-MOF-1	3D	CO_2	107 (195 K)	16

References

1. APEX3. Ver. 2017.3-0. Bruker AXS Inc., Madison, Wisconsin, USA, **2017**.
2. L. Krause, R. Herbst-Irmer, G. M. Sheldrick and D. Stalke, *J. Appl. Cryst.* **2015**, 48, 3-10.
3. XPREP Ver. 2014/2, Bruker AXS Inc., Madison, Wisconsin, USA, **2014**.
4. G. Sheldrick, *Acta Cryst. A* **2015**, 71, 3-8.
5. G. Sheldrick, *Acta Cryst. C* **2015**, 71, 3-8.
6. O. V. Dolomanov, L. J. Bourhis, R. J. Gildea, J. A. K. Howard, H. Puschmann, *J. Appl. Cryst.* **2009**, 42, 339-341.
7. B. H. Toby, R. B. Von Dreele, *J. Appl. Cryst.* **2013**, 46, 544-549.
8. N. Klein, H. C. Hoffmann, A. Cadiau, J. Getzschmann, M. R. Lohe, S. Paasch, T. Heydenreich, K. Adil, I. Senkovska, E. Brunner, *J. Mater. Chem.*, **2012**, 22, 10303-10312.
9. S. Shimomura, M. Higuchi, R. Matsuda, K. Yoneda, Y. Hijikata, Y. Kubota, Y. Mita, J. Kim, M. Takata, S. Kitagawa, *Nat. Chem.*, **2010**, 2, 633.
10. J. A. Mason, J. Oktawiec, M. K. Taylor, M. R. Hudson, J. Rodriguez, J. E. Bachman, M. I. Gonzalez, A. Cervellino, A. Guagliardi, C. M. Brown, *Nature*, **2015**, 527, 357.
11. H. Kajiro, A. Kondo, K. Kaneko, H. Kanoh, *Int. J. Mol. Sci.*, **2010**, 11, 3803-3845.
12. E. R. Engel, A. Jouaiti, C. X. Bezuidenhout, M. W. Hosseini, L. J. Barbour, *Angew. Chem. Int. Ed.* **2017**, *56*, 8874-8878.
13. D. Tanaka, K. Nakagawa, M. Higuchi, S. Horike, Y. Kubota, T. C. Kobayashi, M. Takata, S. Kitagawa, *Angew. Chem.*, **2008**, 120, 3978-3982.
14. K. Fukuhara, S.-i. Noro, K. Sugimoto, T. Akutagawa, K. Kubo, T. Nakamura, *Inorg. Chem.*, **2013**, 52, 4229-4237.
15. X.-M. Liu, R.-B. Lin, J.-P. Zhang, X.-M. Chen, *Inorg. Chem.*, **2012**, 51, 5686-5692.
16. P. Kanoo, R. Haldar, S. K. Reddy, A. Hazra, S. Bonakala, R. Matsuda, S. Kitagawa, S. Balasubramanian, T. K. Maji, *Chem. Eur. J.*, **2016**, 22, 15864-15873.